Fracton excitation and Lévy flight dynamics in alkali silicate glasses

Junko Habasaki and Isao Okada
Tokyo Institute of Technology at Nagatsuta, Yokohama 226, Japan

Yasuaki Hiwatari
Kanazawa University, Kanazawa 920-11, Japan
(Received 6 September 1996)

We have examined the relaxation behavior of alkali metal ions in lithium metasilicate glasses by means of molecular dynamics simulation. We have observed a change of slope of the mean squared displacement at ~300 ps. In shorter time regions, localized motion of lithium ions within neighboring sites is observed, which is caused by the small fracton dimension (fracton excitation). On the other hand, an accelerated motion of particles due to cooperative jumps is found, which characterizes the diffusion and conduction mechanisms of the alkali metal ions in longer time regions. The dynamics of accelerated motion is discussed in relation to Lévy flight dynamics. [S0163-1829(97)03510-8]

I. INTRODUCTION

In a previous work, we investigated the relaxation behavior of atoms in lithium metasilicate glasses by means of molecular dynamics (MD) simulation.[1] Now, attention is focused on the dynamics of lithium ions. We have found that α relaxation process (in several tens to ~ 300 ps region) in Li_2SiO_3 glass can be represented by the stretched exponential-type decay $F_s(k,t)=A\exp[-(t/\tau)^{\beta}]$, where τ is proportional to $\mathbf{k}^{-n}$. The value n is known to be 2 in the Debye-type decay. We have found that n is less than 2 in a glassy state. The β values of Li for $F_s(\mathbf{k},t)$ in the glassy state is less than 1 as usually observed in glasses, which means a slowing down of the dynamics. The low value of n suggests that there exists an accelerated diffusion process that explains the high conductivity of lithium containing glass in spite of overall slowing down of the dynamics.

In the present work, we have performed a longer time simulation up to the 1 ns region, to clarify the dynamics for decreasing n value, since we can expect that such components with accelerated dynamics becomes more remarkable at the longer time region. The role of cooperative motions of atoms forms a key feature to the understanding of the dynamics of diffusion and conduction of alkali metal ions in the long time region.

On the other hand, in short time behavior, the localized motion of the ion is dominant. Fractal dimension analysis has been used to characterize these motions, which are restricted by the structure of the jump paths. The local and global structures of the jump path are important to characterize the short and long time behavior, respectively.

II. MD SIMULATION

MD simulation has been performed in the same way as in previous studies:[1–4] the numbers of the particles in the basic cube being 144 for Li, 72 for Si, and 216 for O. The volume was fixed at that derived by the NPT (constant pressure and temperature) ensemble simulation. The glass transition temperature is approximately 830 K. A Gilbert-Ida-type pair potential function[5] plus an r^{-6} term was used. The parameters of the potential used have previously been derived on the basis of *ab initio* MO (molecular orbital) calculation,[4] and their validity has been checked in the liquid, glassy and crystal states under constant pressure conditions. The run up to 1 ns (250 000 steps) has been performed with the different initial configuration from the previously used one.

III. RESULT AND DISCUSSIONS

A. Mean square displacement and density correlation function

In Fig. 1, the mean squared displacement (MSD) $R2(t)$, of lithium ions is plotted. The change of the slope at ~300 ps is found.

The corresponding density correlation function (self part) $F_s(k,t)$ is shown in Fig. 2. The function is defined as

$$F_s(k,t)=\left\langle \sum_{j=1}^{N_{\alpha'}} \exp\{i\mathbf{k}\cdot d\mathbf{r}_j^{\alpha'}(t)\} \right\rangle \Big/ N_{\alpha'}, \qquad (1)$$

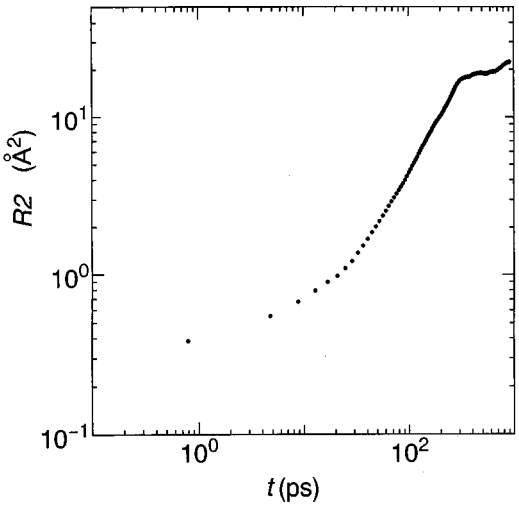

FIG. 1. Log-log plot of the mean square displacement of lithium ions at 700 K.

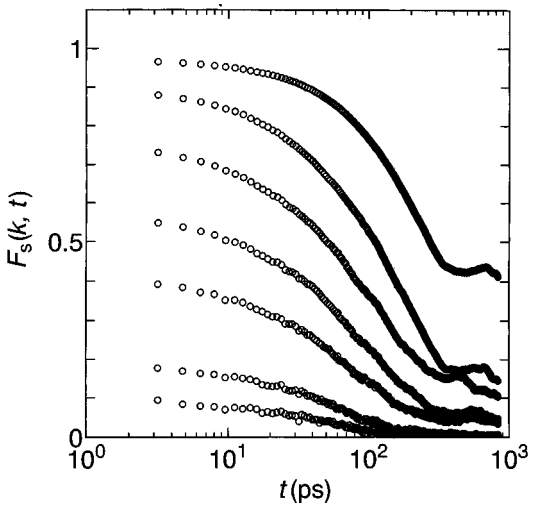

FIG. 2. Density correlation function (self-part) of Li at 700 K. The curves from top to bottom are for wave numbers $k=2\pi/n'$ ($n'=10,5,3,2,1.5,1$, and 0.8) in the unit of Å^{-1}.

where α' denotes the species indices, and $\langle\cdots\rangle$ denotes an initial time average. The function also shows the changes in slopes at several hundred ps. In region after 200 ps, the obtained $F_s(k,t)$ values for each $\mathbf{k}$ are slightly different from those obtained previously[1] from different runs. The cause of such differences will be discussed later.

We call hereafter the region before and after 300 ps $\alpha 1$ and $\alpha 2$, respectively. In the previous work,[1] the α relaxation process was analyzed at $\sim$ 300 ps region, and the fitted parameters thus obtained were for the mixture of several components in these two regions.

To calculate $R2(t)$ in the percolation system,[7] we average over all starting points of the walkers that are uniformly distributed over all sites. If we start in clusters of fixed size s, we can obtain $R2_s(t)$ of a random walker on an s-site cluster. The mean radius R_s of all clusters of s sites is related to s by

$$s \sim R_s^{d_f}. \tag{2}$$

As long as the distance travelled by the random walkers is smaller than R_s, diffusion is anomalous and $R2_s(t) \sim t^{2/d_w}$, where d_f and d_w are fractal dimensions of the jump path and of random walk, respectively. Then we can write

$$R2_s(t) \sim t^{2/d_w}, \tag{3}$$

if $t^{2/d_w} < R_s^2$, where d_w contains the effect of the contribution of waiting time distribution.

For longer times, the random walker cannot escape the s cluster, and $R2_s(t)$ is bounded by R_s^2:

$$R2_s(t) \sim R_s^2 \tag{4}$$

if $t^{2/d_w} > R_s^2$

The change of the slope found in Fig. 1 (at $\sim$18 Å^2) clearly corresponds to the squared value of the first minimum distance of the pair correlation function of the Li-Li pair $[g_{\text{Li-Li}}(r)]$ (4.2 Å).

We have divided the walkers into two components. The walkers in component A show squared displacement less than R_s^2 ($s=2$) during a 1-ns run. Namely, the component is located within neighboring sites. The other walkers in component B show squared displacement larger than R_s^2 during the 1-ns run. Namely, they contribute to the diffusion of long time limit.

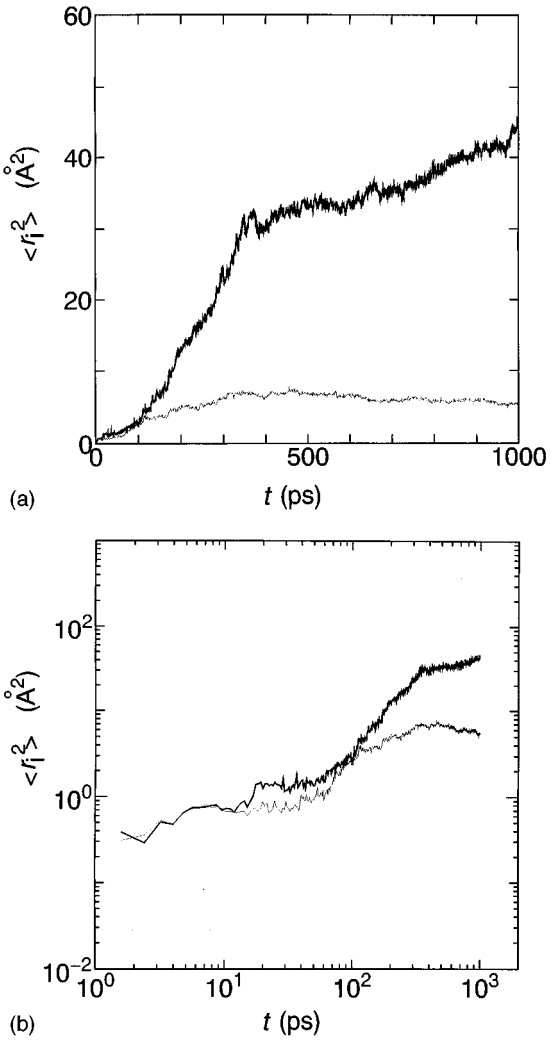

FIG. 3. (a) Linear and (b) log-log plot of the mean square displacement of lithium ions in component A (thin line) and B (thick line) during 1 ns at 700 K.

In Figs. 3(a) and 3(b), both components are plotted on linear and log-log scales, respectively. The mean squared displacement of the component A shows a maximum and does not show large contribution to the long time diffusive behavior. The mean squared displacement in $\alpha 1$ region is the mean value of those for components A and B.

The difference of these two components can be explained by the structure of the jump path and by the existence of both single and cooperative jumps. The jump path of lithium has been found to be low dimensional in localized regions, while the path forms three dimensional percolation clusters.[3] We have assumed the behavior in region $\alpha 1$ is mainly caused by single jump trapped by low-dimensional localized path, while the behavior in region $\alpha 2$ is mainly caused by cooperative jump diffusion traveling three-dimensional connections of these paths, because the characteristic lengths of these motions are different.

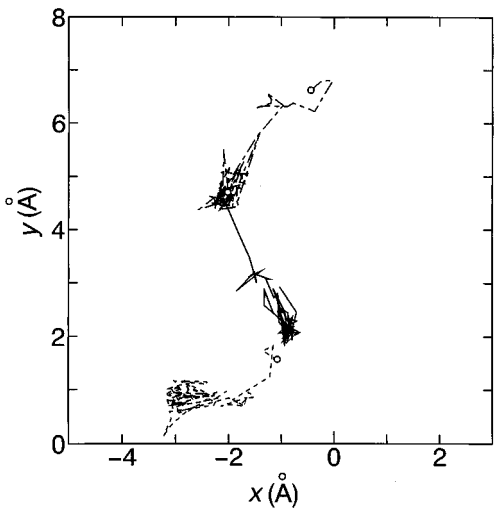

FIG. 4. Trajectories of the lithium ions showing cooperative jumps projected on the x-y plane during 16 ps at 700 K.

To confirm this assumption, we have examined the contributions of the single jumps and cooperative jumps to the squared displacement. Positions of lithium ions are checked every 2 ps during arbitrarily chosen 16 ps. The motion with displacement larger than half distance of the first peak (2.77/2 Å) of the $g_{\text{Li-Li}}(r)$ is defined as a jump. The jumps simultaneously occurring (or within 2 ps in some cases) at neighboring sites are judged to be cooperative. Figure 4 shows an example of cooperative jumps, where three lithium ions jump to the next site at the same time. We have shown that an activation energy of the second ion in cooperative jumps tends to become smaller than that in the single jumps.[3] In Table I, the numbers of cooperative jumps and the contribution of these motions to mean squared displacements are given. As seen from this Table, even in a short period, the contribution of cooperative motion to the mean squared displacement is quite large in spite of a small number of events of cooperative jumps. We have also confirmed that all ions traveling longer distances than first minimum of the $g_{\text{Li-Li}}(r)$ are concerned with the cooperative jumps, at least in this time scale. Therefore, the ions causing cooperative motion must become the main component in long time region.

B. Fractal dimension analysis

The d_f for the local (0.7 $\sim$ 2.0 Å) region is found to be less than 1 (0.22, obtained from the plot of averaged positions of every 0.4 ps during 16 ps run) for this system at 700 K. The value less than 1 means the existence of long life component and the local path of low dimension. However, the structure of the jump path of Li in Li_2SiO_3 in longer range is found to be three dimensional ($d_f c = 2.98$, where c means for clustering region). Therefore, localization is not due to structure of the cluster but designates due to local structure of low dimension as discussed below.

The value of d_w is directly obtained from the trajectories[3] during 1 ns to avoid the effect of waiting time distribution of the jump motions. The values d_w for the component A and B are found to be 2.83 and 2.47, respectively. Both values are greater than 2 (the value for the free random walk): A higher value for A means that the ions in component A tend to be trapped more in the low-dimensional structure.

A combination of the large d_w and small d_f values means a localized motion (fracton excitation). Fractal time distribution of jump motion[1] also contributes to the time-dependent behavior. Namely, both components with long life and with high back correlated motion contribute to the slowing down of the decay of $F_s(\mathbf{k},t)$. The combination of the temporal and spatial mechanism is thoretically treated by Blumen *et al.*[6] These two mechanisms are distinguishable in a microscopic point of view. Results of further analysis of these mechanisms will be shown in a separate paper.

C. Fracton excitation

Low dimension of the jump path causes a localization of the single jump of the particles as follows. Alexander and Orbach[9] have argued the vibrational excitations related to the ''fracton dimension.''

The linear size of the region of sites visited by the walker after N steps is

TABLE I. Contribution of cooperative jumps. (a) Number of single and cooperative jumps during arbitrarily chosen 16 ps. (b) Square displacements of the alkali metal ions during the 16 ps.

	(a)	
System	Type	Number of event
Li_2SiO_3 (700 K)	Li → Li →	6
	Li → Li → Li →	2
	5Li →[a]	1
	Li →	17

	(b)		
	Square displacements (Å^2)		Ratio (%)
System	total	Cooperative	cooperative to total
Li_2SiO_3 (700 K)			
Li	211.3	166.2	79

[a]Complicated collective motion of 5 ions.

$$\langle R2(N)\rangle^{1/2}\sim N^{1/d_w}. \tag{5}$$

The number of visited sites $V(N)$ becomes

$$V(N)\sim R^{D_f}\sim N^{\tilde{d}/2}, \tag{6}$$

where the fracton dimension $\tilde{d}$ is defined by

$$\tilde{d}=\frac{2d_f}{d_w}. \tag{7}$$

The probability $\langle P_0(t)\rangle$ of finding the particle at the origin at time t is given as follows, if the particle was located at the origin at time $t=0$:

$$\langle P_0(N)\rangle\sim[V(N)]^{-1}. \tag{8}$$

Here we have used N instead of t, to remove the effect of waiting time distribution of jump motions. Thus the single jump cannot have a large contribution to the diffusion nor conduction due to the large back correlation probability.

D. Lévy flight dynamics

On the other hand, the mean squared displacement of the component B increases sharply in the 50–300 ps region. The slope in the log-log plot during this period is 1.77, which means that $R2(t)$ for this component increases faster than t linear. That is, the component B shows the accelerated dynamics at least in this time region, which corresponds to the small n value in the wave number dependence of $F_s(k,t)$.

The accelerated dynamics observed cannot be explained merely by the overlap of components with different s values. Such behavior is explained by cooperative motion (jumps in glassy state) of lithium ions,[3] because the path of backward jump for an ion is intercepted by the simultaneous jump of an ion which follows.

The behavior of the cooperative jumps seems to be quite similar to that observed in the kicked rotor or in Josephson junctions, where the accelerated dynamics has been found.[8] The dynamics is named after Lévy. Lévy flights are widely applied in nonlinear, fractal, chaotic, and turbulent systems. Below is described the essence of the Lévy flight dynamics.[8]

Brownian motion is essentially characterized by a Gaussian probability distribution of the position of the random walker after a time t, with the variance proportional to t. When we consider an N-step random walk in one dimension, the probability $P_N(X)$ for the sum of N steps $X=X_1+X_2+X_3+\cdots+X_N$ has the same Gaussian distribution $p(x)$ as the individual steps, because a sum of N Gaussians is again a Gaussian. However, Cauchy found other solutions to the N-step addition of random variables. The form for the probability when it is Fourier transformed from real x space to reciprocal $\mathbf{k}$ space is given by

$$p_N(k)=\exp[-Nk^{\beta}]. \tag{9}$$

In the Gaussian case, $p_N(\mathrm{k})$ is equal to $\exp[-Nk^2]$. These random walks with steps with infinite second moments are known to be Lévy flights. A special example of random walk in one dimension can be written in the form

$$p(x)=\frac{\lambda-1}{2\lambda}\sum_{j=0}^{\infty}\lambda^{-j}(\delta_{(x,+b^j)}+\delta_{(x,-b^j)}), \tag{10}$$

where $\delta_{(x,y)}$ means the Kronecker δ. Jumps of size 1, b, b^2, and so on can occur, but jumps of an order of magnitude longer in base b occur an order of magnitude less often in base λ. Taking the Fourier transform of $p(x)$, we obtain the Weierstrass function, namely,

$$\tilde{p}(k)=\frac{\lambda-1}{2\lambda}\sum_{j=0}^{\infty}\lambda^{-j}\cos(b^j\mathbf{k}). \tag{11}$$

For the random walk process, the final result in the form

$$\tilde{p}(k)\sim\exp[-Nk^{\alpha'}], \tag{12}$$

with $\alpha'=\ln\lambda/\ln$ b is obtained, where $\langle x^2\rangle$ becomes infinite for $\alpha'<2$. The form is the same as in Eq. (9). The value α' represents the fractal dimension of a random walk path.

In random-work displacement in Brownian motion grows only in proportion to the square root of time. However, the displacement in Lévy flights grows faster than Brownian motion, as just observed for the component B. The smaller value of d_w of component B than A can also be explained by the contribution of small d_w value of Lévy flight dynamics.

When the cooperative jumps occur, the path of back-correlated jump for the first ion is intercepted by the second ion, which occupies the original site of the first ion. Thus the component of cooperative jumps should have a larger forward correlation probability than the single jumps. Thus the acceleration of the dynamics is explained by the existence of the cooperative jumps.

As seen in Table I, the cooperative jumps occur less frequently if a larger number of lithium ions are involved. A nearly linear line (with slope of -1.8) is obtained from the log-log plot of this relation. This result shows that the cooperative jumps on longer scales occur in a fractal manner. If the characteristic length of n-correlated jumps is b^n, the situation is just the same as discussed above for the special example, where b is the characteristic length for the single jump. Equation (13) is obtained by applying an inverse Fourier transform to Eq. (12):

$$p_n(x)\sim\mathrm{const}\times n/x^{1+\alpha'}. \tag{13}$$

As pointed out by Shlesinger *et al.*, the sums with $\alpha'<2$ are dominated by their largest terms, hence by rare intermittent events. This feature is important for an understanding of the mechanism of the reproducibility of dynamics in a limited time simulation. The difference between the run I and II can be attributed to such characteristics of the cooperative jumps.

E. Relationship between fracton excitation and Lévy flight dynamics

The typical behavior of Li ions in each component A and B is shown in Fig. 5. A comparison of groups A and B reveals that without such accelerated dynamics, the walker cannot escape from the nearest-neighbor region, because the corresponding backward jump would follow with the high probability in the single jump mechanism. That is, a particle

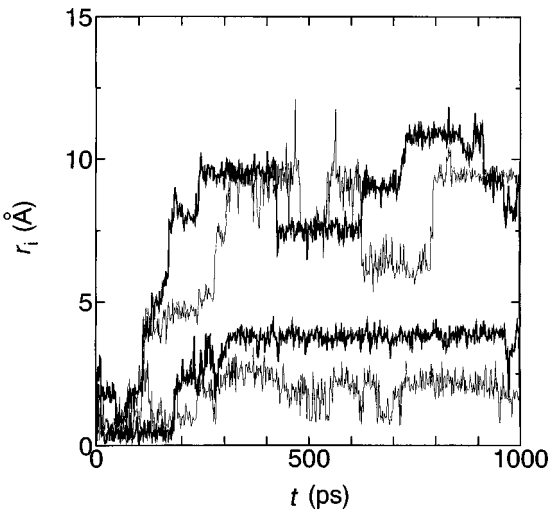

FIG. 5. Some examples of displacement r_i of Li ions are plotted against time during 1-ns run at 700 K. Upper two curves are for the particles which belong to component B, and lower ones are for those which belong to component A.

moving within a local network can switch from time to time to a motion along a global network by forward correlated jumps caused by the cooperative motion. Three-dimensional connection of the jump paths is efficient to cause the diffusion and conduction when the particle can escape from the nearest-neighbor region. The particles of component B escaping from the localized motion may be trapped in other sites in the hierarchic manner, since the definition of these components depends on the choice of t_0.

In Fig. 6, the observed displacement, r_i of each lithium ion after nth jumps from the position at $t=0$ is plotted against the angle of jump (θ) measured from the previous jump vector. Trajectories are measured by the scale of half distance of the first peak (2.77/2 Å) of the $g_{\text{Li-Li}}(r)$. Two components are clearly found in the figure. Behavior of square displacement of each lithium ion $r2$ can be represented by the following equation using the mean angle of the jump θ, if the jump length s is a constant:

$$r2(n)=ns^2+\sum_{i,j} s_i s_j = ns^2\left(1+(1/n)\sum \cos\theta_{ij}\right). \quad (14)$$

The plot of r_i versus θ for each n distributes randomly (or in chaotic manner) in a liquid state. Therefore, the mean value of $\cos\theta$ becomes 0. In contrast, the similar plot at 700 K as shown in Fig. 6(a) clearly shows the two regions correspond to two kinds of dynamics. The component at around $\theta/2\pi=0.2$ tends to jump with forward correlation. On the other hand, the component at around $\theta/2\pi=0.5$ is for ions located within the nearest-neighbor sites. Therefore the main feature of dynamics in glassy state can be characterized by the strain of these angles and accelerated dynamics can be partly characterized by the limited angles.

Since such motions are made at random by the back-correlated motions, the second moment of $\langle x^2\rangle$ is not infinite in this case. Distribution of waiting time distribution, namely the fractal time, may also overcome the divergence in $\langle x^2\rangle$; such a process is named Lévy walks by Shlesinger *et al.*[8]

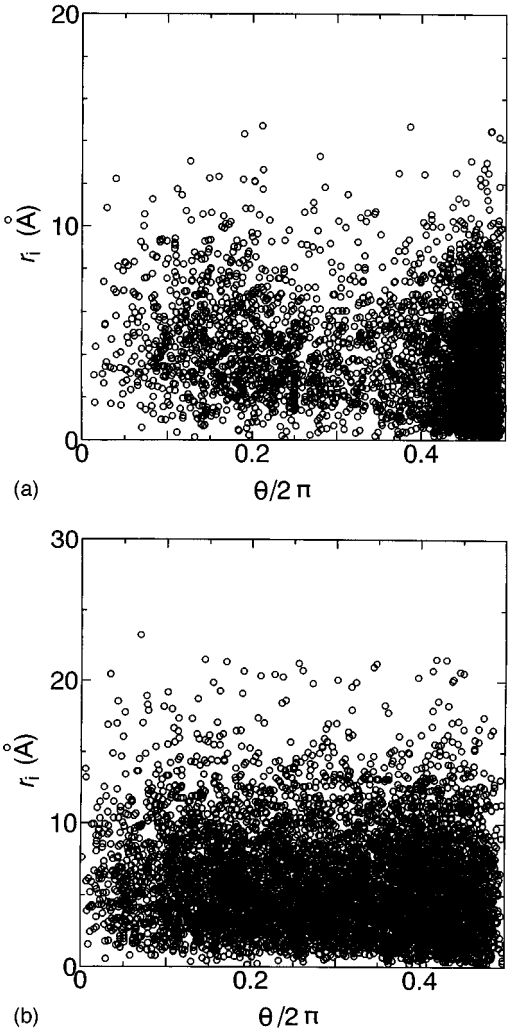

FIG. 6. The displacement r_i is plotted against θ, where the trajectories are checked by using the scale length λ. [λ is chosen as of the half length of the first maximum of $g_{\text{Li-Li}}(r)$.] (a) at 700 K during the 1-ns run, (b) at 2000 K during 16 ps run.

Distribution of displacement of lithium ion r_i during a 1 ns run is plotted in Fig. 7. The particle with large r_i is considered to have repeated the accelerated jumps. The number of lithium ions having large r_i is found to decrease in a fractal manner. It is also found that the contribution of smaller number of events with larger r_i to total displacement tends to be larger in a large r_i region. These features are also expected for the Lévy flight dynamics.

This tendency is also observed in Fig. 7(b) for liquid, where a low value of n has been observed while no restricted angle is observed. Therefore, the cause of accelerated dynamics is not only the limited angles but also the distribution of characteristic length. As shown in these figures, the large motion of lithium can be characterized by the component showing Lévy flight dynamics.

F. Universal dynamic response in glass

In general, the frequency dependence of ionic conductivity σ of glass can be represented by the sum of a frequency-independent or dc region and a frequency-dependent power-law region.

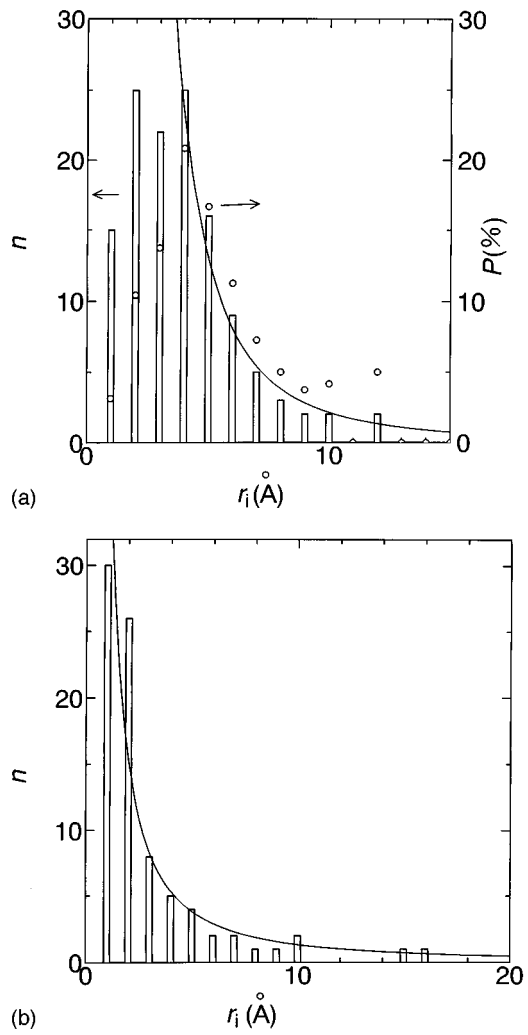

FIG. 7. Distribution of displacement r_i of Li (a) at 700 K during 1 ns, (b) at 2000 K during 16 ps. Contribution of r_i to the total displacement is also shown in (a). The fitted curves in the form $n \sim r_i^b$, are shown [(a): $b=-2.62$ (b): $b=-1.52$].

$$\sigma = \sigma_{\mathrm{dc}} + A\omega^{s'}, \tag{15}$$

where A and s' are empirical constants. Such behavior is called ''universal dynamic response'' or ''universal dielectric response'' as far as the permittivity and the conductivity are concerned. Maass *et al.*[10] have pointed out that the power law in the dynamic response is related to strong backward correlation among subsequent hops of ions. Funke[11] has reviewed the recent development of studies related to the jump relaxation in solid electrolytes. The dispersive hopping conductivity is interpreted in terms of ''unsuccessful'' forward-backward hopping sequences. The stretched exponential function is often regarded as the signature of the ''universal dynamic response.'' The relationship between the power laws and the stretched exponential behavior for the simple jump relaxation model is also discussed by Funke.[11]

Elliott[12] has argued that there are two general mechanisms that can lead to an ac conductivity exhibiting power-law frequency dependence. The first is a parallel conduction process, in which the ionic hopping events causing relaxation are independent and have a distribution of relaxation times. Odagaki[13] has also argued the power-law behavior in stochastic transport in the trapping diffusion model with a distribution of the jump rate.

Both features are quite similar to those just observed for the A component mainly due to single jump motion. Namely, both waiting time distribution and strong back-correlation due to fracton excitation contribute to the power-law behavior in the high-frequency ($\alpha 1$) region.

The other approach argued by Elliott[12] is based on a series conduction process, in which constrained relaxation occurs; a given site can only relax when a certain event occurs at another site with which it is coupled. The component of cooperative motions of like ions also contributes in this time region as already discussed, although the microscopic mechanism suggested by him is not consistent with our results.

On the other hand, in the $\alpha 2$ region, the cooperative jumps become a main component, which determine the long time behavior of the mean squared displacement. This component is considered to contribute to main dc conductance in a longer time region.

Two stage relaxation processes ($\alpha 1$ and $\alpha 2$) exist in many systems. In his review, Funke referred to experimental evidence of a superposition of two processes (although it is not easy to detect) found in some ion conducting glasses.

Thus the universal dynamic response in glass is explained by the combination of the contributions of single and cooperative jumps. Cooperative motions of atoms have been observed even in the MD simulation for soft core glasses,[14] which have no rigid framework structures. Furthermore, the universal dynamic response is widely observed in glasses, semiconductors, and so on. Therefore, the accelerated dynamics and the fracton excitation observed in the present system is not just a special example. The underlying general mechanism for the present system can explain various behavior in other systems.

IV. CONCLUSION

This is a report on evidence of the Lévy flight dynamics in a glass system. Cooperative jump motion causes enhancement of forward correlated jumps leading to accelerated dynamics. On the other hand, single jump in local low-dimensional network structure tends to be localized and shows the ''fracton excitation.'' A combination of these two motions explains the universal response of the dynamics observed widely in glasses and semiconductors.

ACKNOWLEDGMENTS

A part of the calculations in this work was performed with HITAC M-680 and S-820 computers at the Institute for Molecular Science at Okazaki and with FACOM VPP500 computer at the Institute for Solid State Physics, University of Tokyo. The CPU time made available is gratefully acknowledged. We thank the Ministry of Education, Science and Culture, Japan (No. 07236103) for financial support.

[1] J. Habasaki, I. Okada, and Y. Hiwatari, Phys. Rev. E **52**, 2681 (1995).
[2] J. Habasaki, I. Okada, and Y. Hiwatari, J. Non-Cryst. Solids **183**, 12 (1995).
[3] J. Habasaki, I. Okada, and Y. Hiwatari, J. Non-Cryst. Solids **208**, 181 (1997).
[4] J. Habasaki and I. Okada, Mol. Simul. **9**, 319 (1992).
[5] Y. Ida, Phys. Earth Planet Interiors **13**, 97 (1976).
[6] A. Blumen, J. Klafter, B. S. White, and G. Zumofen, Phys. Rev. Lett. **53**, 1301 (1984).
[7] S. Halvin and D. Ben-Avraham, Adv. Phys. **36**, 695 (1987).
[8] M. F. Shlesinger, G. M. Zaslavsky, and J. Klafter, Nature (London) **363**, 31 (1993); J. Klafter, M. F. Shledinger, and G. Zumofen, Phys. Today **49** (2), 33 (1996).
[9] S. Alexander and R. Orbach, J. Phys. (Paris) Lett. **43**, L625 (1982).
[10] P. Maass, J. Petersen, A. Bunde, W. Dieterich, and H. E. Roman, Phys. Rev. Lett. **66**, 52 (1991).
[11] K. Funke, Prog. Solid St. Chem. **22**, 111 (1993).
[12] S. R. Elliott, Solid State Ionics **27**, 131 (1988).
[13] K. Odagaki, Phys. Rev. B **38**, 9044 (1988).
[14] H. Miyagawa, Y. Hiwatari, B. Bernu, and J. P. Hansen, J. Chem. Phys. **88**, 3879 (1988).